Novel near-infrared luminescent hybrid materials covalently linking with lanthanide [Nd(III), Er(III), Yb(III), and Sm(III)] complexes via a primary β-diketone ligand: synthesis an...

ARTICLE *in* THE JOURNAL OF PHYSICAL CHEMISTRY C · JULY 2009

Impact Factor: 4.77

Novel Near-Infrared Luminescent Hybrid Materials Covalently Linking with Lanthanide [Nd(III), Er(III), Yb(III), and Sm(III)] Complexes via a Primary β-Diketone Ligand: Synthesis and Photophysical Studies

Xianmin Guo,[†,‡] Huadong Guo,[†,‡] Lianshe Fu,[§] L. D. Carlos,[§] R. A. S. Ferreira,[§] Lining Sun,[†,‡] Ruiping Deng,[†] and Hongjie Zhang*[,†]

State Key Laboratory of Rare Earth Resource Utilizations, Changchun Institute of Applied Chemistry, Chinese Academy of Sciences, 5625 Renmin Street, Changchun 130022, People's Republic of China, Graduate School of the Chinese Academy of Sciences, People's Republic of China, and Department of Physics, CICECO, University of Aveiro, 3810-193 Aveiro, Portugal

Received: January 18, 2009; Revised Manuscript Received: May 6, 2009

A series of novel, colorless, and transparent sol−gel derived hybrid materials Ln-DBM-Si covalently grafted with $Ln(DBM-OH)_3 \cdot 2H_2O$ (where DBM−OH = *o*-hydroxydibenzoylmethane, Ln = Nd, Er, Yb, and Sm) were prepared through the primary β-diketone ligand DBM−OH. The structures and optical properties of Ln-DBM-Si were studied in detail. The investigation results revealed that the lanthanide complexes were successfully in situ grafted into the corresponding hybrids Ln-DBM-Si. Upon excitation at the maximum absorption of ligands, the resultant materials displayed excellent near-infrared luminescence. Meanwhile, a model for the indirect excitation mechanism was introduced to discuss the ligands-to-Ln^{3+} intramolecular energy transfer. Furthermore, the radiative properties of the Nd^{3+} ion and the Er^{3+} ion in Ln-DBM-Si are evaluated by applying the Judd-Ofelt analysis.

Introduction

Recently, the large degree of attention has been focused on the investigation of near-infrared (NIR) luminescence of trivalent lanthanide (Ln) ions, for example, neodymium (Nd^{3+}),[1] erbium (Er^{3+})[2] and ytterbium (Yb^{3+})[3] switching from the traditional visible europium (Eu^{3+})[4] and terbium (Tb^{3+})[5] luminescence. The driving forces are mainly stemmed from the requirements of vivo imaging,[6] laser systems,[7] optical amplifiers,[8] or light-emitting diodes[9] in the telecommunications industry. Since lanthanide ions are very poor at absorbing light directly because of the low extinction coefficients of the Laporte-forbidden f−f transitions, it is difficult to generate efficient luminescence by direct excitation of these NIR luminescent lanthanide ions. To improve absorption, the lanthanide ions are usually chelated with an adjacent strongly absorbing chromophore in the UV region. Upon ultraviolet light irradiation, the central lanthanide ions display the characteristic luminescence originating from the effective intramolecular energy transfer through the excited state of the ligand to the emitting level of the lanthanide ion (the so-called "antenna effect").[10−12] As it is well-known, lanthanide β-diketonate complexes are useful molecular luminescent materials, which have attracted considerable attention due to highly efficient emission bands of the ligands, long radiative lifetimes of the excited state, and high luminescence quantum efficiency.[13−15] However, for practical applications, it is advantageous to fabricate the supposed "organic−inorganic hybrid materials (OIHs)" by incorporation of luminescent lanthanide complexes into an inert host matrix (e.g., silica-based materials,[16−19] polymers,[20] or liquid crystals[21]) to improve their photo- and thermal stabilities.

The sol−gel process is one of the preferred synthetic routes for the preparation of OIHs used in integrated optics circuits. The major advantages of the process are its simplicity, mild reaction conditions, and ability to control the purity and homogeneity of the final materials at the nanomolecular scale.[22] Meanwhile, the method offers the possibility of tailoring the final properties of the materials, for instance, the refractive index, phonon energy, and transparency through the suitable choice of the organic and inorganic components.[23−27] Generally, two main routes have been used to introduce lanthanide complexes into sol−gel derived materials:[18f] (1) direct dissolution or dispersion of lanthanide complexes in the sol−gel hosts through weak interactions, such as van der Waals contacts, hydrogen bonding, or electrostatic forces[28,29] and (2) attachment of the lanthanide complexes to the sol−gel matrix through strong chemical bonds, such as covalent, iono-covalent, or Lewis acid−base bonds.[17,19] The first approach offers the advantage of versatility, through which both the sol−gel matrix and the lanthanide complex can be chosen independently, but it is difficult to obtain a uniform distribution of the lanthanide complexes in sol−gel materials due to their clustering, low solubility, and/or poor stability in the sol−gel precursor solutions. In contrast, the homogeneously dispersed transparent monolithic composite materials can be obtained by the second method, avoiding the self-quenching resulting from the concentration effect.

Therefore, in this manuscript, we synthesized a series of colorless, transparent, and homogeneous hybrid materials containing NIR lanthanide complexes via a functionalized primary ligand *o*-hydroxydibenzoylmethane (DBM−OH) using the sol−gel process. At the same time, we have carried out detailed studies of NIR luminescence properties of the obtained hybrid materials. Moreover, the ligands-to-Ln^{3+} energy transfer

* To whom correspondence should be addressed. Fax: +86-431-85698041. E-mail: hongjie@ciac.jl.cn.
† Changchun Institute of Applied Chemistry, Chinese Academy of Sciences.
‡ Graduate School of the Chinese Academy of Sciences.
§ University of Aveiro.

10.1021/jp9005179 CCC: $40.75
Published on Web 06/16/2009

was also investigated. The optical properties of Nd^{3+} and Er^{3+} ions in the corresponding hybrids were also evaluated using the Judd-Ofelt theory.[30]

Experimental Section

Materials. 3-Isocyanatepropyltriethoxysilane (ICPTES), *o*-hydroxyacetophenone, benzoyl chloride, tetraethoxysilane (TEOS), potassium hydroxide (KOH), hydrochloric acid (HCl), and *N*,*N*-dimethylformamide (DMF) were commercially available and used without purification. Petroleum ether, triethylamine, pyridine, tetrahydrofuran (THF), and ethanol (EtOH) were all distilled before use. Lanthanide(III) chloride ($LnCl_3 \cdot 6H_2O$; Ln = Nd, Er, Yb, and Sm) was obtained by reaction of the corresponding lanthanide oxide (Ln_2O_3, 99.99%) with HCl and dissolved in EtOH. All reagents were of analytic grade and purchased from Beijing Chemical Factory except that ICPTES was bought from Aldrich. Distilled water was used throughout the experiments.

Synthesis of the Precursor Containing Dibenzoylmethane (DBM-Si). The starting reagent DBM−OH was synthesized according to a known procedure,[31] and characterized by ^{1}H NMR and FTIR spectra. DBM-Si was prepared as follows: triethylamine (10 mmol) and ICPTES (15 mmol) were added under nitrogen to a solution of DBM−OH (10 mmol) in anhydrous THF (10 mL). The mixture was heated at reflux for 24 h and then added dropwise into petroleum ether under stirring. The resulting white precipitate was filtered off, washed with petroleum ether for 4 times, and dried at 50 °C in vacuum for 10 h. The resulting DBM-Si was characterized by ^{1}H NMR spectrum. ^{1}H NMR (DMSO, 400 MHz) δ (ppm): 16.12 (1H, s, OH of enol), 8.40 (1H, t, NH), 8.13−8.17 (1H, dd, ArH), 7.90−7.93 (3H, m, ArH), 7.80−7.82 (1H, d, ArH), 7.57−7.65 (5H, m, ArH and CH of enol), 3.77 (6H, q, OCH_2), 3.08 (2H, q, NCH_2), 1.46 (2H, quint, CH_2), 1.20 (9H, t, CH_3), 0.53 (2H, t, $SiCH_2$). Elemental analysis: Calculated: C, 61.60%; H, 6.78%; N, 2.87%. Found: C, 61.52%; H, 6.75%; N, 2.92%.

Synthesis of Hybrid Materials Covalently Bonded with Lanthanide Complex via DBM−OH Ligand (Ln-DBM-Si, Ln = Nd, Er, Yb, and Sm). Ln-DBM-Si hybrid materials were prepared as follows: the molar ratio of TEOS/EtOH/H_2O (0.01 M HCl) in original solution was 1:4:4. Then, an appropriate amount of DBM-Si was introduced into the solution. Upon resulting clear sol, $LnCl_3$ ethanol solution was added with a molar ratio of Ln^{3+}/DBM-Si = 1:3 and the concentration of the Eu^{3+} ions was Ln^{3+}/Si = 0.5 mol %. The mixed solution was agitated magnetically for several hours at room temperature to obtain a single phase and then transferred to a plastic container with some holes on the cover. During the conversion process of sol to monolithic xerogel, the binary Ln complex was in situ synthesized accompanied with the evaporation of HCl and ethanol. The precursor solution converted to colorless transparent monolithic gel after several days of drying at 40 °C. The resulting hybrid materials were denoted as Ln-DBM-Si. The detail synthetic procedure and the possible structure for Ln-DBM-Si are shown in Scheme 1.

Characterization. Fourier transform infrared spectra (FTIR) were measured on a Bruker Vertex 70 spectrophotometer within the wavenumber range 4000−400 cm^{-1} at a resolution of 4 cm^{-1} using KBr pressed pellet technique. Diffuse reflectance UV−visible (DR UV−vis) spectra were acquired from Hitachi F-4100 with tungsten and deuterium lamps. The fluorescence excitation and emission spectra were recorded on a JY FL-3 spectrophotometer at the liquid nitrogen temperature (77 K) equipped with a 450 W xenon lamp as an excitation source.

SCHEME 1: Schematic Diagram of Synthetic Procedure and the Possible Structure for the Hybrid Materials Ln-DBM-Si

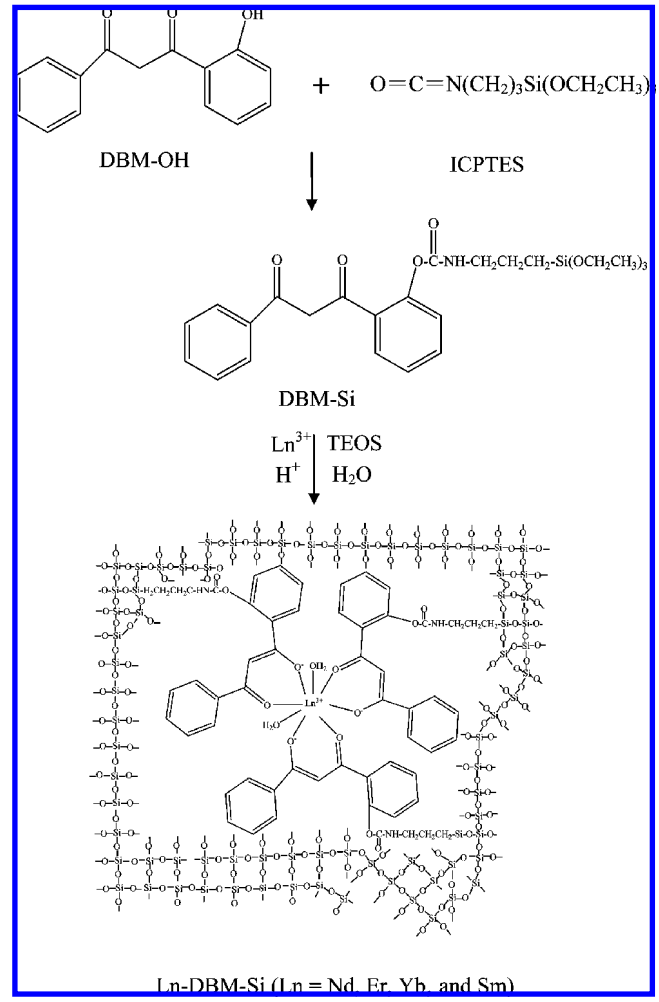

Luminescence lifetime was measured with a Lecroy Wave Runner 6100 digital oscilloscope (1 GHz) using different wavenumber lasers (Continuum Sunlite OPO with pulse width = 4 ns) as an excitation source. The samples, Nd-DBM-Si and Er-DBM-Si, with dimensions of 1.96 and 1.77 cm in diameter and 0.23 and 0.34 cm in thickness, respectively, were applied to the optical absorption measurements. The spectral optical densities $OD(\lambda) = 0.4343 l\rho\sigma(\lambda)$ of Nd-DBM-Si and Er-DBM-Si were recorded at room temperature using a Sihmadzu UV-3101 PC. The corresponding concentration is 4.94×10^{19} Nd/cm^3 and 4.58×10^{19} Er/cm^3. All measurements were performed at room temperature except the fluorescence spectra and lifetimes.

Results and Discussion

Local Structure. The FTIR spectra of DBM-Si (a), Nd-DBM-Si (b), and Er-DBM-Si (c) are shown in Figure 1. For the spectrum of ligand DBM-Si (Figure 1a), the bands at 1535, 1632, 1647 (ν, CONH), 1765 (ν, O−C═O), and 1397 cm^{-1} (ν, C−N) suggest the success of the grafting of DBM−OH on the molecule of ICPTES. A strong broadband located at 2970 cm^{-1} originates from the three methylene groups of 3-(triethoxysilyl)propyl isocyanate.[32] In addition, the spectrum of DBM-Si is dominated by ν(C−Si, 1191 cm^{-1}) and ν(Si-OEt, 1070 cm^{-1}) absorption bands, characteristic of trialkoxysilyl functions. In

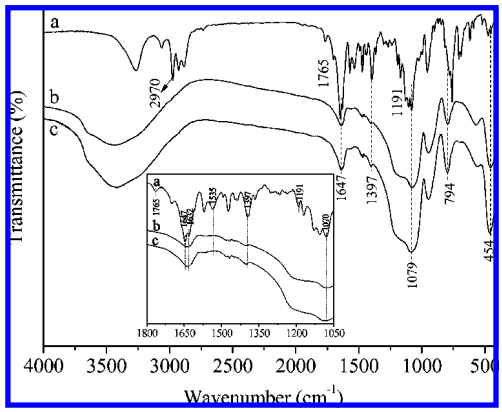

Figure 1. FTIR spectra of DBM-Si (a), Nd-DBM-Si (b), and Er-DBM-Si (c).

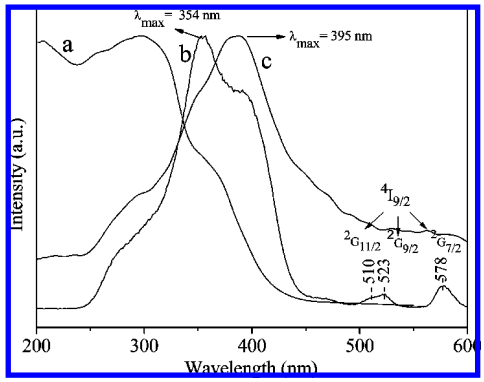

Figure 2. DR UV−vis absorption spectrum of DBM-Si (a) in the solid; excitation spectra for Nd-DBM-Si (b) and Er-DBM-Si (c) monitored at 1060 and 1535 nm in the solid, respectively. All spectra are normalized to a constant intensity at the maximum.

the curves of Figure 1b, c the formation of Si−O−Si framework is evidenced by the peaks located at 1079 cm^{-1} (ν_{as}, Si−O−Si), 794 cm^{-1} (ν_s, Si−O−Si), and 454 cm^{-1} (δ, Si−O−Si) (ν = stretching, δ = in-plane bending, s = symmetric, and as = asymmetric vibrations), respectively. Furthermore, the peaks at 1637, 1540, and 1400 cm^{-1} in curves b and c of Figure 1, originating from the amide groups and C−N of the −CONH group of DBM-Si, can be still observed in the obtained hybrid materials, suggesting the fact that DBM-Si remains intact after the hydrolysis/condensation reaction. However, the absorption bands corresponding to the stretching vibration of Nd−O or Er−O were not clearly observed in the curves b and c of Figure 1, which is perhaps due to the relatively lower concentration of Ln^{3+} (Ln = Nd and Er) in the hybrid materials or the shielding of the surrounding host. The similar phenomenon was also observed in other work.[19] Since other FTIR spectra of Ln-DBM-Si (Ln = Yb and Sm) are similar to those of the above two hybrid materials, their FTIR spectra are not shown in this section but are presented in Supporting Information (Figure S1).

Luminescence Properties. The excitation spectra of the obtained materials Ln-DBM-Si (Ln = Nd and Er, monitored at 1060 and 1535 nm, respectively) and DR UV−vis absorption spectrum of DBM-Si are displayed in Figure 2. The overlaps can be observed between the excitation bands of Ln-DBM-Si (b for Nd-DBM-Si and c for Er-DBM-Si) and the absorption band of DBM-Si (a), which indicates that in the hybrids the central Ln^{3+} ion can be efficiently sensitized by the ligand through the so-called antenna effect.[33] Consequently, we can come to the conclusion that the intramolecular energy transfer in hybrid materials occurs between the DBM-Si and the Ln^{3+} ions. The other overlaps between the excitation spectra of the resulting Ln-DBM-Si (Ln = Yb and Sm) and the absorption spectrum of the ligand DBM-Si, which are provided in Supporting Information (Figure S2), also imply that the Ln^{3+} ions in the hybrid materials can be efficiently sensitized by the ligand DBM-Si.

In the normalized excitation spectrum of Nd-DBM-Si (b in Figure 2), a broad excitation band in the range of 235 to 490 nm (λ_{max} = 355 nm) and some low relative intensity peaks are observed, which can be assigned to the $\pi-\pi^*$ electron transition of the organic ligand and the characteristic absorption transitions of the Nd^{3+} ion, respectively. These f−f transitions are ascribed to $^4I_{9/2} \rightarrow {}^2G_{11/2}$ (510 nm), $^4I_{9/2} \rightarrow {}^2G_{9/2}$ (523 nm), and $^4I_{9/2} \rightarrow {}^2G_{7/2}$ (578 nm) of Nd^{3+} ion. Compared with the absorption intensity of organic ligand, these absorption transitions are too weak, proving that luminescence sensitization via excitation of ligand is much more efficient than direct excitation of the absorption levels of the Nd^{3+} ions. For the excitation spectrum of Er-DBM-Si (c in Figure 2), it also displays a broad excitation band in the UV region due to the absorption of DBM-Si ligand. Similarly, for other excitation spectra of Yb-DBM-Si and Sm-DBM-Si (Figure S2), a broad excitation band owing to the absorption of organic ligand emerges from 230 to 550 nm by monitoring the corresponding maximum emission wavelength of the Ln^{3+} ions.

The normalized emission spectra in the near-infrared region for Ln-DBM-Si (Ln = Nd, Er, Yb, and Sm) are presented in Figure 3 under 355−395 nm excitation wavelength. For the Nd hybrid material, the emission spectrum consists of three bands at 897, 1060, and 1330 nm, attributed to the $^4F_{3/2} \rightarrow {}^4I_{9/2,11/2,13/2}$ transitions, respectively.[34] The strongest emission of Nd^{3+} ion is centered at around 1060 nm, and the intense emission band constitutes approximately 72% of the total emission intensity. Nd-containing systems have been regarded as the most popular infrared luminescent materials for application in laser systems (the basis of the common 1064 nm laser). Meanwhile, the Nd^{3+} ion is also ideally suitable as the optically active component because of the development of the optical amplifier at 1300 nm.[21b,35] Therefore, the resulting Nd-DBM-Si provides an opportunity to develop new materials suitable for the laser applications and optical amplifiers.

For the Er^{3+}-based hybrid, an observed emission band in the range of 1450 to 1700 nm with a 74 nm full width at half-maximum (fwhm) centered at 1535 nm is ascribed to the $^4I_{13/2} \rightarrow {}^4I_{15/2}$ transition, which enables a wide gain bandwidth for optical amplifications in comparison with that of other similar Er^{3+}-doped material.[29a] Therefore, Er-DBM-Si may be potentially served as the gain medium in lasers and optical amplifiers operating at the standard telecommunications wavelength of 1540 nm.

For the Yb^{3+} hybrid, the typical $^2F_{5/2} \rightarrow {}^2F_{7/2}$ transition at 980 nm was detected, which has been proposed as a promising probe for fluoroimmuno-assays and vivo applications.[3] It is worth noting that the Yb^{3+} ion emission band is not a single sharp transition but an envelope of bands arising at lower energies than the primary 980 nm band, which results from the crystal field splitting. A similar phenomenon has also been reported in the previous literatures.[36]

For the Sm hybrid, the most intense emission band can be observed at 942 nm, which is assigned to the transition $^4G_{5/2} \rightarrow {}^6F_{5/2}$, as a potential time-resolved material. The other emissions are ascribed to the transitions from the $^4G_{5/2}$ excited level to the $^6H_{13/2}$ (786 nm), $^6F_{3/2}$ (906 nm), $^6F_{5/2}$ (942 nm), $^6F_{7/2}$ (1023 nm), $^6F_{9/2}$ (1168 nm), and $^6F_{11/2}$ (1378 nm) states. It should be

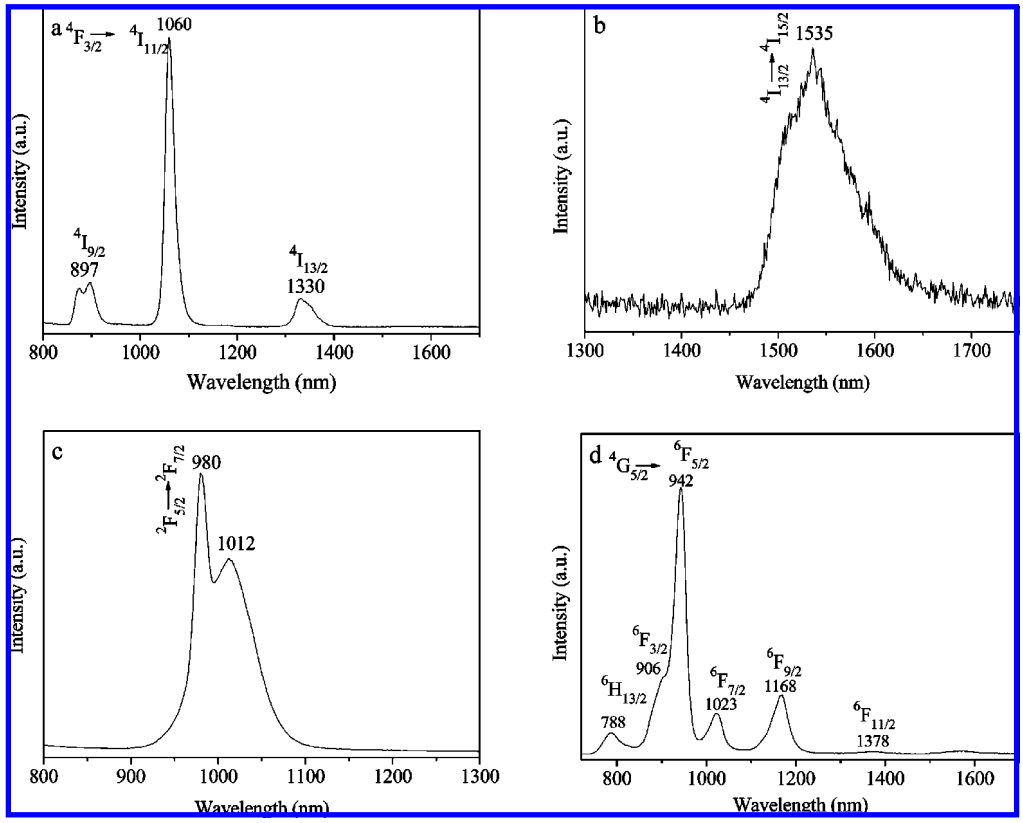

Figure 3. Normalized emission spectra for Ln-DBM-Si, Ln = Nd (a, λ_{ex} = 355 nm), Er (b, λ_{ex} = 385 nm) Yb (c, λ_{ex} = 395 nm), and Sm (d, λ_{ex} = 355 nm).

noted that the visible emissions for Sm hybrid are also detected at 563, 598, 645, and 705 nm, which are attributed to the $^4G_{5/2} \rightarrow {}^6H_{5/2,7/2,9/2,11/2}$ transitions, respectively (Figure S3).

Energy Transfer Mechanism. The triplet state energy level of DBM-Si ligands was determined from the phosphorescence spectrum of the respective Gd^{3+} complex because of their enhanced phosphorescence−fluorescence ratio ($\Phi_p/\Phi_f > 100$) compared with those of other Ln chelate complexes at 77 K under UV excitation. The triplet state energy level of DBM-Si is determined to be 20 325 cm^{-1} from the corresponding shortest-wavelength phosphorescence band, which is assumed to be the 0−0 transition of the ligand. According to Dexter's theory,[37] the suitability of the energy difference between the resonance level of the Ln^{3+} ion and the triplet state of the ligand is a critical factor for efficient energy transfer.[10b] The too large or too small energy difference both decrease the efficient ligand-to-metal ion energy transfers.[38] As described above, we obtained a series of the characteristic Ln^{3+} ion NIR emission spectra upon excitation at the maximum of the excitation spectra in Ln-DBM-Si hybrids. This indicates the following: (i) the ligands (DBM-Si) can shield the Ln^{3+} ions well from their surroundings and transfer the absorbed energy from their triplet states to the central metal Ln^{3+} ions, an antenna effect, which is in agreement with the excitation results mentioned above (Figure 2); (ii) complex is formed between the Ln^{3+} ions and the ligands during the conversion in situ synthesis process of sol to xerogel. According to the discussion above, a model for the indirect excitation mechanism is suggested and shown as a schematic energy diagram in Scheme 2. Furthermore, the 4f energy levels of the Ln^{3+} ions are also depicted on the right of Scheme 2.

For the Nd-DBM-Si hybrid, since the energy of the $^4G_{9/2}$ excited state is ~19 400 cm^{-1}, the ligands can transfer its energy to this state and then a nonradiative decay from the $^4G_{9/2}$ level

SCHEME 2: Model for the Main Pathways in the Sensitization Process (Left) and Schematic Energy Diagram of the 4f Levels of the Ln^{3+} Ions (Ln = Nd, Er, Yb, and Sm; Right)

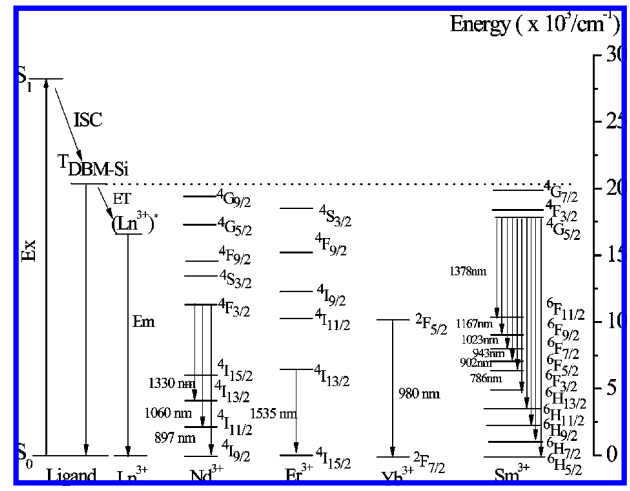

populates the $^4F_{3/2}$ level (11 400 cm^{-1}) originating the characteristic Nd^{3+} NIR luminescence. For the Er-DBM-Si hybrid, no visible emission was discerned, and the $^4I_{13/2}$ level (~6 500 cm^{-1}) is populated by nonradiative decay from the $^4S_{3/2}$ state (~18 300 cm^{-1}) originating the characteristic Er^{3+} NIR luminescence. For the Yb-DBM-Si hybrid, the large energy difference between the triplet state of DBM-Si (20 325 cm^{-1}) and the resonance $^2F_{5/2}$ level (10 235 cm^{-1}) of Yb^{3+} eliminates any possible energy matching, as has been proposed by Khreis et al.[39] Thus, the sensitive mechanism from ligand-to-Yb^{3+} is

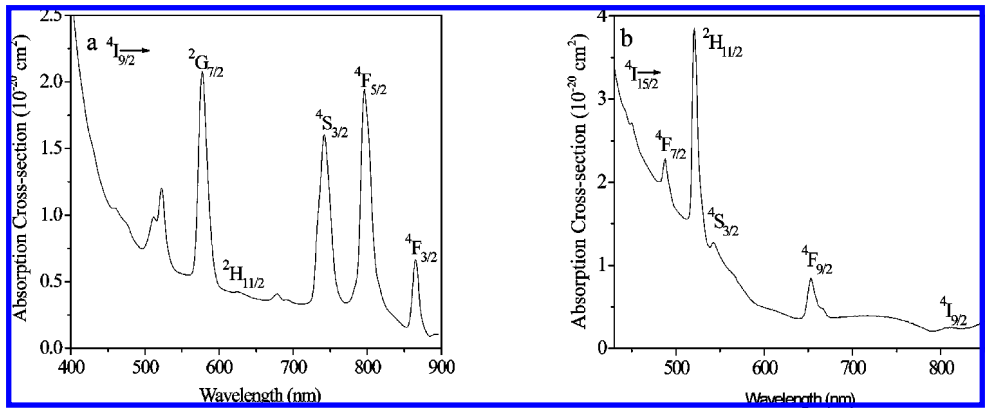

Figure 4. Absorption spectra of Nd-DBM-Si (a) and Er-DBM-Si (b).

different from the antenna effect, which may occur via phonon-assisted energy-transfer process pointed out by Güdel and co-workers.[40]

For the Sm-DBM-Si hybrid, there are three Sm^{3+} excited states, $^4G_{7/2}$ (~20 050 cm^{-1}), $^4F_{3/2}$ (~18 700 cm^{-1}), and $^4G_{5/2}$ (~17 700 cm^{-1}), that can receive energy from the lowest triplet state of the ligand (~20 325 cm^{-1}). However, intense emission is only observed from the $^4G_{5/2}$ level. The reason for this is the close proximity of these three excited states to each other, which causes electrons from the higher states to rapidly relax nonradiatively to the $^4G_{5/2}$ level, from which radiative transitions occur.[41]

In addition, the time-resolved measurements on the Ln-DBM-Si materials (Ln = Nd, Er, Yb, and Sm) were carried out under liquid-nitrogen-cooled conditions by using an excitation wavelength of 355 nm and monitored around the most intense emission line of their corresponding emission spectra. The luminescence decay profiles for Ln-DBM-Si (not shown) are all well-fitted with single exponentials, suggesting that the Ln^{3+} ions are located in the same average local environment in each hybrid material. The corresponding lifetimes of the $^4F_{3/2}$ (Nd-DBM-Si, 1060 nm), $^4I_{13/2}$ (Er-DBM-Si, 1535 nm), $^2F_{5/2}$ (Yb-DBM-Si, 980 nm), and $^4G_{5/2}$ (Sm-DBM-Si, 942 nm) levels are 54, 77, 245, and 573 ns, respectively. Compared with other similar hybrid materials,[29] the lower luminescent decay time values observed for Ln-DBM-Si hybrids may be attributed to the fact that the nonradiative (k_{nr}) transition probability is higher in Ln-DBM-Si hybrid materials.

Judd-Ofelt Analysis. As discussed above, the Nd-DBM-Si and Er-DBM-Si hybrid materials have the possibility to develop the laser systems and optical amplifiers. To further evaluate the potential of Ln-doped materials, it is essential to study the radiative properties of the sol−gel hybrid materials. As is well-known, the Judd-Ofelt (J-O) theory[30] is one of the most successful theories to analyze the radiative transition within the $4f^N$ configuration of a trivalent Ln ion in host matrix based on its room temperature optical absorption measurement.

Figure 4 exhibits the absorption spectra of Nd-DBM-Si and Er-DBM-Si in the UV−vis-NIR region. The spectra show the characteristic optical absorption bands of Nd^{3+} and Er^{3+} ions, corresponding to electron transitions from the ground ($^4I_{9/2}$ for Nd^{3+} and $^4I_{15/2}$ for Er^{3+}) multiplet to the upper energy states. Five Nd^{3+} ion or Er^{3+} ion absorption bands in the corresponding absorption spectra were selected to determine the phenomenological oscillator strength parameters. The band positions along with assignments in the absorption spectra are shown in Table 1 and Table 2. Accordingly, the measured line strength S_{mea} and the calculated line strengths S_{cal} of the five absorption bands

TABLE 1: Assignments of the Absorption Bands, Measured and Calculated Line Strengths of Nd^{3+} Ion in Nd-DBM-Si[a]

level	λ (nm)	S_{mea} ($\times 10^{-20}$ cm^2)	S_{cal} ($\times 10^{-20}$ cm^2)
$^2G_{7/2}$	578	3.0539	3.0534
$^2H_{11/2}$	624	0.0323	0.0658
$^4S_{3/2}$	742	2.4071	2.4969
$^4F_{5/2}$	798	2.6880	2.5745
$^4F_{3/2}$	866	0.4895	0.5870

[a] All transitions are from the $^4I_{9/2}$ state.

TABLE 2: Assignments of the Absorption Bands, Measured and Calculated Line Strengths of Er^{3+} Ion in Er-DBM-Si[b]

level	λ (nm)	S_{mea} ($\times 10^{-20}$ cm^2)	S_{cal} ($\times 10^{-20}$ cm^2)
$^4F_{7/2}$	488	0.7860	0.8011
$^2H_{11/2}$	522	4.3563	4.3515
$^4S_{3/2}$	544	0.2071	0.2277
$^4F_{9/2}$	653	1.0842	1.0432
$^4I_{9/2}$	807	0.0952	0.1939

[b] All transitions are from the $^4I_{15/2}$ state.

TABLE 3: Judd-Ofelt Intensity Parameters of Nd^{3+} Ion in Nd-DBM-Si and Er^{3+} Ion in Er-DBM-Si

samples	Ω_2 ($\times 10^{-20}$ cm^2)	Ω_4 ($\times 10^{-20}$ cm^2)	Ω_6 ($\times 10^{-20}$ cm^2)
Nd-DBM-Si	35.05	1.20	5.68
Er-DBM-Si	5.36	1.06	1.03

can be obtained using the formula in the literature,[42,43] which are separately tabulated in Table 1 and Table 2. Meanwhile, the oscillator strength parameters Ω_λ (λ = 2, 4, 6) can be obtained using the formula in the literature (results listed in Table 3).[44]

Up to now, the interpretation of the physical meaning of the phenomenological oscillator-strength parameters remains controversial. Ω_2 is usually a reflection of local structure and related to the degree of covalence in the lanthanide-first-coordination-shell interaction.[43b,45] The large Ω_2 value for Nd-DBM-Si and a comparable Ω_2 value for Er-DBM-Si imply the presence of covalent bonding between the lanthanide ions and the vicinity ligands, as is reasonable.[18g,46]

Furthermore, the quality of the fit can be characterized by root-mean-square (rms) deviation of the experimental and calculated line strengths, which is defined by

$$rms\Delta S = \sqrt{\sum_{i=1}^{N} (S_{mea} - S_{cal})^2/(N-3)} \qquad (1)$$

TABLE 4: Calculated Transition Probability, Fluorescence Branching Ratio, Radiative Lifetime, and Stimulated Emission Cross-Section of Nd^{3+} in Nd-DBM-Si

transitions	λ (nm)	S_{cal} ($\times 10^{-20}$ cm^2)	A (s^{-1})	β_c	σ_e ($\times 10^{-21}$ cm^2)	τ_R (ms)
$^4F_{3/2} \rightarrow {}^4I_{9/2}$	896	0.5864	177.8	0.290	0.96	
$^4F_{3/2} \rightarrow {}^4I_{11/2}$	1060	2.4674	359.8	0.587	7.77	1.63
$^4F_{3/2} \rightarrow {}^4I_{13/2}$	1330	1.1843	75.1	0.132	2.13	

TABLE 5: Calculated Transition Probability, Radiative Lifetime, and Stimulated Emission Cross-Section of Er^{3+} in Er-DBM-Si

transition	λ (nm)	S_{cal} ($\times 10^{-20}$ cm^2)	A (s^{-1})	τ_R (ms)	σ_e ($\times 10^{-21}$ cm^2)
$^4I_{13/2} \rightarrow {}^4I_{15/2}$	1536	1.7034	68.7	14.56	1.94

where N is the number of absorption bands analyzed. A measurement of the relative error of the fit is given by the rms error = rmsΔS/rms$S \times 100\%$, where rms$S = \sqrt{\sum(S_{mea}{}^2)/(N)}$. The corresponding rms error of the fitting is 5.6% and 3.8%, which indicates that the fitting results are in good agreement with the experiments.[47]

In addition, the parameters Ω_λ are generally used to determine the radiative transition probabilities A from the initial state $\mathbf{J}_{|(S,L)J\rangle}$ to the terminal state $\mathbf{J'}_{|(S',L')J'\rangle}$ of the emissive transitions. Therefore, A can be calculated by the equation in the literature:[42a]

$$A = \frac{64\pi^4 e^2}{3h(2J+1)\bar{\lambda}^{-3}} \frac{n(n^2+2)^2}{9} \sum_{t=2,4,6} \Omega_t |\langle (S,L)J \| U^t \| (S',L')J' \rangle|^2 \quad (2)$$

According to the spontaneous transition probability A, the radiative lifetimes for the excited $^4I_{9/2}$, $^4I_{11/2}$, and $^4I_{13/2}$ state of Nd^{3+} ion, and $^4I_{13/2}$ state of Er^{3+} ion are determined using equation[48]

$$\tau_R = \frac{1}{\sum A} \quad (3)$$

which represents an effective average over site-to-site variations in the local rare earth environment. Based on the value for the spontaneous transition probability and corresponding emission spectrum, the stimulated emission cross-section σ_e is separately obtained on the basis of the following expression:[42a]

$$\sigma_e = \frac{A\lambda^2}{4\pi^2 n^2 \Delta\nu} \quad (4)$$

Thus, the calculated line strengths S_{cal} of emissive transition, the radiative transition rate, the calculated radiative lifetime, and the stimulated emission cross-section for Nd and Er ions are also listed in Table 4 and Table 5, respectively.

It can be easily seen that the calculated radiative lifetimes for Nd-DBM-Si (1.63 ms) and Er-DBM-Si (14.56 ms) are comparable with those of Nd-doped or Er-doped glass systems that have been used to make lasers and optical amplifiers.[49] At the same time, the above radiative lifetimes values are much higher than those of the hybrids that our group has reported previously,[29] which indicates that Nd-DBM-Si hybrid and Er-DBM-Si hybrid are efficient for laser pumping.

In the aspect of the stimulated emission cross-section, σ_e of the $4F_{3/2} \rightarrow {}^4I_{11/2}$ fluorescence transition of Nd^{3+} ion is one of the most important parameters for laser design, which is dependent only on Ω_4 and Ω_6 due to the triangle rule $|J - J'| \leq \lambda \leq (J + J')$, $\|U^{(t)}\|^2 = 0$, $t = 2$.[42a] In our case, the value for Nd-DBM-Si in the 1060 nm transition and that for Er-DBM-Si in the 1536 nm transition are of the same order of magnitude as those for Nd^{3+}-doped and Er^{3+}-doped glass systems,[49] which indicates that the $^4F_{3/2} \rightarrow {}^4I_{11/2}$ transition of the Nd^{3+} ion in the Nd-DBM-Si can be considered as a possible laser transition and that Er-DBM-Si with the wide fwhm (74 nm) discussed above has the possibility to develop a tunable laser and a broadband optical amplifier in the 1.54 μm wavelength region.

In addition, for Nd-DBM-Si, the radiative transition rate represents the total transition probability for radiative decay from the initial manifold. Thus, the fluorescence branching rations (β) can be determined from the radiative decay rates by the formula[42a]

$$\beta[(S,L)J;(S',L')J'] = \frac{A[(S,L)J;(S',L')J']}{\sum_{S',L',J'} A[(S,L)J;(S',L')J']} \quad (5)$$

The corresponding values are tabulated in Table 4. As well-known, β is a critical parameter to the laser designer, because it characterizes the possibility of attaining stimulated emission from any specific transition. It can be shown that the possibility of $^4F_{3/2} \rightarrow {}^4I_{11/2}$ transition is the largest among three transitions.

Conclusions

A series of transparent, homogeneous, and colorless hybrid materials Ln-DBM-Si were synthesized by covalently bonding with a binary lanthanide complex Ln(DBM−OH)$_3$ (Ln = Nd, Er, Yb, and Sm) via a β-diketone primary ligand. The optical properties of the Ln-DBM-Si were investigated in detail. Upon excitation of the ligand absorption bands, the corresponding Ln-DBM-Si materials display the characteristic NIR luminescence, mediated by the sensitizing effect of the ligands in hybrid materials, a well-known antenna effect. The perfect emission band at 1330 nm for Nd-DBM-Si and the broad emission band at 1535 nm for Er-DBM-Si provide the opportunities to develop new materials suitable for optical amplifiers operating at 1.3 and 1.5 μm, the two telecommunications windows. The highly intense emission band at 1060 nm for Nd-DBM-Si offers the possible application in laser systems (the basis of the common 1064 nm laser). The strong emission band at 980 nm for Yb-DBM-Si may be as a promising probe for fluoroimmuno-assays and in vivo applications. In addition, the absorption spectra for Nd-DBM-Si and Er-DBM-Si are also investigated in detail. According to the J-O theory, a series of experimental parameters were calculated and analyzed, such as radiative transition rates and emission cross sections. The above radiative lifetime values of Nd-DBM-Si and Er-DBM-Si are much higher than those of the hybrid materials that our group has previously reported, indicating that Nd-DBM-Si and Er-DBM-Si are efficient for laser pumping. From the research results, we believe our method can provide a new way to prepare multicomposite hybrid

materials for lasers, fluoroimmuno-assays, and optical amplification applications.

Acknowledgment. This project is financially supported by the National Natural Science Foundation of China (Grants 20490210, 206301040, and 20602035) and the MOST of China (Grants 2006CB601103, 2006DFA42610). L.S.F. expresses his gratitude to the Fundação para a Ciência e a Tecnologia (Portugal) for the financial support of this work.

Supporting Information Available: FTIR spectra of Yb-DBM-Si and Sm-DBM-Si, excitation spectra of Yb-DBM-Si and Sm-DBM-Si, and emission spectrum of Sm-DBM-Si in the visible region. This material is available free of charge via the Internet at http://pubs.acs.org.

References and Notes

(1) (a) Beeby, A.; Faulkner, S. *Chem. Phys. Lett.* **1997**, *266*, 116. (b) Klink, S. I.; Alink, P. O.; Grave, L.; Peters, F. G. A.; Hofstraat, J. W.; Geurts, F.; van Veggel, F. C. J. M. *J. Chem. Soc.-Perkin Trans.* **2001**, *2*, 363. (c) Hebbink, G. A.; Klink, S. I.; Grave, L.; Alink, P. G. B. O.; van Veggel, F. C. J. M. *Chem. Phys. Chem.* **2002**, *3*, 1014. (d) Imbert, D.; Cantuel, M.; Bünzli, J.-C. G.; Bernardinelli, G.; Piguet, C. *J. Am. Chem. Soc.* **2003**, *125*, 15698.

(2) (a) Wang, H. S.; Qian, G. D.; Wang, M. Q.; Zhang, J. H.; Luo, Y. S. *J. Phys. Chem. B* **2004**, *108*, 8084. (b) Song, L. M.; Liu, X. H.; Zhen, Z.; Chen, C.; Zhang, D. M. *J. Mater. Chem.* **2007**, *17*, 4586.

(3) (a) Beeby, A.; Dickins, R. S.; Faulkner, S.; Parker, D.; Williams, J. A. G. *Chem. Commun.* **1997**, 1401. (b) Werts, M. H. V.; Hofstraat, J. W.; Geurts, F. A. J.; Verhoeven, J. W. *Chem. Phys. Lett.* **1997**, *276*, 196.

(4) (a) Parker, D.; Senanayake, K.; Williams, J. A. G. *Chem. Commun.* **1997**, 1777. (b) Batista, H. J.; de Andrade, A. V. M.; Longo, R. L.; Simas, A. M.; de Sa, G. F.; Ito, N. K.; Thompson, L. C. *Inorg. Chem.* **1998**, *37*, 3542. (c) Wang, L. H.; Wang, W.; Zhang, W. G.; Kang, E. T.; Huang, W. *Chem. Mater.* **2000**, *12*, 2212.

(5) (a) Bruce, J. I.; Dickins, R. S.; Govenlock, L. J.; Gunnlaugsson, T.; Lopinski, S.; Lowe, M. P.; Parker, D; Peacock, R. D.; Perry, J. J. B.; Aime, S.; Botta, M. *J. Am. Chem. Soc.* **2000**, *122*, 9674. (b) Dutton, P. J.; Conte, L. *Langmuir* **1999**, *15*, 613.

(6) (a) Licha, K. Contrast agents for optical imaging. *Top. Curr. Chem.* **2002**, *222*, 1. (b) Prata, M. I. M.; Santos, A. C.; Torres, S.; André, J. P.; Martins, J. A.; Neves, M.; García-Martín, M. L.; Rodrigues, T. B.; López-Larrubia, P.; Cerdán, S.; Geraldes, C. F. G. C. *Contrast Media and Molecular Imaging* **2006**, *1*, 246. (c) Voisin, P.; Ribot, E. J.; Miraux, S.; Bouzier-Sore, A. K.; Lahitte, J. F.; Bouchaud, V.; Mornet, S.; Thiaudière, E.; Franconi, J. M.; Raison, L.; Labrugère, C.; Delville, M. H. *Bioconjugate Chem.* **2007**, *18*, 1053.

(7) (a) Iwamuro, M.; Hasegawa, Y.; Wada, Y.; Murakoshi, K.; Kitamura, T.; Nakashima, N.; Yamanaka, T.; Yanagida, S. *Chem. Lett.* **1997**, 1067. (b) Hasegawa, Y.; Ohkubo, T.; Sogabe, K.; Kawamura, Y.; Wada, Y.; Nakashima, N.; Yanagida, S. *Angew. Chem., Int. Ed.* **2000**, *39*, 357. (c) Meinardi, F.; Colombi, N.; Destri, S.; Porzio, W.; Blumstengel, S.; Cerminara, M.; Tubino, R. *Synth. Met.* **2003**, *137*, 959.

(8) (a) Hebbink, G. A.; Stouwdam, J. W.; Reinhoudt, D. N.; Van Veggel, F. C. J. M. *Adv. Mater.* **2002**, *14*, 1147. (b) Slooff, L. H.; van Blaaderen, A.; Polman, A.; Hebbink, G. A.; Klink, S. I.; Van Veggel, F. C. J. M.; Reinhoudt, D. N.; Hofstraat, J. W. *J. Appl. Phys.* **2002**, *91*, 3955. (c) Bünzli, J.-C. G.; Piguet, C. *Chem. Soc. Rev.* **2005**, *34*, 1048.

(9) Kang, T. S.; Harrison, B. S.; Bouguettaya, M.; Foley, T. J.; Boncella, J. M.; Schanze, K. S.; Reynolds, J. R. *Adv. Funct. Mater.* **2003**, *13*, 205.

(10) (a) Weissman, S. I. *J. Chem. Phys.* **1942**, *10*, 214. (b) Sato, S.; Wada, M. *Bull. Chem. Soc. Jpn.* **1970**, *43*, 1955. (c) De Sá, G. F.; Malta, O. L.; De Mello Donegá, C.; Simas, A. M.; Longo, R. L.; Santa-Cruz, P. A.; da Silva, E. F., Jr. *Coord. Chem. Rev.* **2000**, *196*, 165. (d) Reisfeld, R. *Struct. Bonding (Berlin)* **2004**, *106*, 209.

(11) Klink, S. I.; Hebbink, G. A.; Grave, L.; van Veggel, F. C. J. M.; Reinhoudt, D. N.; Slooff, L. H.; Polman, A.; Hofstraat, J. W. *J. Appl. Phys.* **1999**, *86*, 1181.

(12) Mancino, G.; Ferguson, A. J.; Beeby, A.; Long, N. J.; Jones, T. S. *J. Am. Chem. Soc.* **2005**, *127*, 524.

(13) (a) Melby, L. R.; Rose, N. J.; Abramson, E.; Caris, J. C. *J. Am. Chem. Soc.* **1964**, *86*, 5117. (b) Bauer, H. J.; Blanc, J.; Ross, D. L. *J. Am. Chem. Soc.* **1964**, *86*, 5125.

(14) (a) Mc Gehee, M. D.; Bergstedt, T.; Zhang, C.; Saab, A. P.; O'Regan, M. B.; Bazan, G. C.; Srdanov, V. I.; Heeger, A. J. *Adv. Mater.* **1999**, *11*, 1349. (b) Yang, C. V.; Srdanov, V.; Robinson, M. R.; Bazan, G. C.; Heeger, A. J. *Adv. Mater.* **2002**, *14*, 980.

(15) (a) Holz, R. C.; Thompson, L. C. *Inorg. Chem.* **1993**, *32*, 5251. (b) Wang, J. F.; Wang, R. Y.; Yang, J.; Zheng, Z. P.; Carducci, M. D.; Cayou, T.; Peyghambarian, N.; Jabbour, G. E. *J. Am. Chem. Soc.* **2001**, *123*, 6179. (c) Shavaleev, N. M.; Pope, S. J. A.; Bell, Z. R.; Faulkner, S.; Ward, M. D. *Dalton Trans.* **2003**, 808. (d) Bassett, A. P.; Magennis, S. W.; Glover, P. B.; Lewis, D. J.; Spencer, N.; Parsons, S.; Williams, R. M.; de Cola, L.; Pikramenou, Z. *J. Am. Chem. Soc.* **2004**, *126*, 9413. (e) Biju, S.; Ambili Raj, D. B.; Reddy, M. L. P.; Kariuki, B. M. *Inorg. Chem.* **2006**, *45*, 10651. (f) Fernandes, J. A.; Braga, S. S.; Pillinger, M.; Ferreira, R. A. S.; Carlos, L. D.; Hazell, A.; Ribeiro-Claro, P.; Goncalves, I. S. *Polyhedron* **2006**, *25*, 1471.

(16) (a) Matthews, L. R.; Kobbe, E. T. *Chem. Mater.* **1993**, *5*, 1697. (b) Embert, F.; Mehdi, A.; Reye, C.; Corriu, R. J. P. *Chem. Mater.* **2001**, *13*, 4542. (c) Franville, A. C.; Zambon, D.; Mahiou, R.; Troin, Y. *Chem. Mater.* **2000**, *12*, 428.

(17) (a) Binnemans, K.; Lenaerts, P.; Driesen, K.; Görller-Walrand, C. *J. Mater. Chem.* **2004**, *14*, 191. (b) Lenaerts, P.; Storms, A.; Mullens, J.; D'Haen, J.; Gorller-Walrand, C.; Binnemans, K.; Driesen, K. *Chem. Mater.* **2005**, *17*, 5194. (c) Driesen, K.; Van Deun, R.; Görller-Walrand, C.; Binnemans, K. *Chem. Mater.* **2004**, *16*, 1531.

(18) (a) de Zea Bermudez, V.; Ferreira, R. A. S.; Carlos, L. D.; Molina, C.; Dahmouche, K.; Ribeiro, S. J. L. *J. Phys. Chem. B* **2001**, *105*, 3378. (b) Carlos, L. D.; Ferreira, R. A. S.; Rainho, J. P.; de Zea Bermudez, V. *Adv. Funct. Mater.* **2002**, *12*, 819. (c) Gago, S.; Fernandes, J. A.; Rainho, J. P.; Ferreira, R. A. S.; Pillinger, M.; Valente, A. A.; Santos, T. M.; Carlos, L. D.; Ribeiro-Claro, P. J. A.; Gonçalves, I. S. *Chem. Mater.* **2005**, *17*, 5077. (d) Lima, P. P.; Ferreira, R. A. S.; Freire, R. O.; Almeida Paz, F. A.; Fu, L. S.; Alves, S., Jr.; Carlos, L. D.; Malta, O. L. *Chem. Phys. Chem.* **2006**, *7*, 735. (e) Fernandes, M.; de Zea Bermudez, V.; Ferreira, R. A. S.; Carlos, L. D.; Charas, A.; Morgado, J.; Silva, M. M.; Smith, M. J. *Chem. Mater.* **2007**, *19*, 3892. (f) Carlos, L. D.; Ferreira, R. A. S.; de Zea Bermudez, V.; Ribeiro, S. J. L. *Adv. Mater.* **2009**, *21*, 509. (g) Molina, C.; Ferreira, R. A. S.; Poirier, G.; Fu, L. S.; Ribeiro, S. J. L.; Messsaddeq, Y.; Carlos, L. D. *J. Phys. Chem. C* **2008**, *112*, 19346.

(19) (a) Li, H. R.; Lin, J.; Zhang, H. J.; Li, H. C.; Fu, L. S.; Meng, Q. G. *Chem. Commun.* **2001**, 1212. (b) Li, H. R.; Lin, J.; Zhang, H. J.; Fu, L. S.; Meng, Q. G.; Wang, S. B. *Chem. Mater.* **2002**, *14*, 3651. (c) Liu, F. Y.; Fu, L. S.; Wang, J.; Meng, Q. G.; Li, H. R.; Guo, J. F.; Zhang, H. J. *New J. Chem.* **2003**, *27*, 233. (d) Li, H. R.; Yu, J. B.; Liu, F. Y.; Zhang, H. J.; Fu, L. S.; Meng, Q. G.; Peng, C. Y.; Lin, J. *New J. Chem.* **2004**, *28*, 1137.

(20) (a) Smirnov, V. A.; Philippova, O. E.; Sukhadolski, G. A.; Khokhlov, A. R. *Macromolecules* **1998**, *31*, 1162. (b) Bekiari, V.; Pistolis, G.; Lianos, P. *Chem. Mater.* **1999**, *11*, 3189. (c) Lenaerts, P.; Driesen, K.; Van Deun, R.; Binnemans, K. *Chem. Mater.* **2005**, *17*, 2148.

(21) (a) Binnemans, K.; Görller-Walrand, C. *Chem. Rev.* **2002**, *102*, 2303. (b) Van Deun, R.; Moors, D.; De Fré, B.; Binnemans, K. *J. Mater. Chem.* **2003**, *13*, 1520. (c) Arenz, S.; Babai, A.; Binnemans, K.; Driesen, K.; Giernoth, R.; Mudring, A. V.; Nockemann, P. *Chem. Phy. Lett.* **2005**, *402*, 75. (d) Nockemann, P.; Beurer, E.; Driesen, K.; Van Deun, R.; Van Hecke, K.; Van Meervelt, L.; Binnemans, K. *Chem. Commun.* **2005**, 4354. (e) Lunstroot, K.; Driesen, K.; Nockemann, P.; Görller-Walrand, C.; Binnemans, K.; Bellayer, S.; Bideau, J. L.; Vioux, A. *Chem. Mater.* **2006**, *18*, 5711.

(22) Hench, L. L.; West, J. K. *Chem. Rev.* **1990**, *90*, 33.

(23) Kojima, K.; Tsuchiya, K.; Wada, N. *J. Sol-Gel Sci. Technol.* **2000**, *19*, 511.

(24) Slooff, L. H.; de Dood, M. J. A.; van Blaaderen, A.; Polman, A. *J. Non-Cryst. Solids* **2001**, *296*, 158.

(25) Ishizaka, T.; Kurokawa, Y. *J. Appl. Phys.* **2001**, *90*, 243.

(26) Chen, S. Y.; Ting, C. C.; Hsieh, W. F. *Thin Solid Films* **2003**, *434*, 171.

(27) Elalamy, Z.; Drouard, E.; Mcgovern, T.; Escoubas, L.; Simon, J. J.; Flory, F. *Opt. Commun.* **2004**, *235*, 365.

(28) Fu, L. S.; Ferreira, R. A. S.; Nobre, S. S.; Carlos, L. D.; Rocha, J. *J. Lumin.* **2007**, *122*, 265.

(29) (a) Sun, L. N.; Zhang, H. J.; Fu, L. S.; Liu, F. Y.; Meng, Q. G.; Peng, C. Y.; Yu, J. B. *Adv. Funct. Mater.* **2005**, *15*, 1041. (b) Sun, L. N.; Zhang, H. J.; Meng, Q. G.; Liu, F. Y.; Fu, L. N.; Peng, C. Y.; Yu, J. B.; Zheng, G. L.; Wang, S. B. *J. Phys. Chem. B* **2005**, *109*, 6174.

(30) (a) Judd, B. R. *Phys. Rev.* **1962**, *127*, 750. (b) Oflet, G. S. *J. Chem. Phys.* **1962**, *37*, 511.

(31) Chen, A. H.; Kuo, W. B.; Chen, C. W. *J. Chin. Chem. Soc.* **2003**, *50*, 123.

(32) Li, Y.; Yan, B.; Yang, H. *J. Phys. Chem. C* **2008**, *112*, 3959.

(33) (a) Sabbatini, N.; Mecati, A.; Guardigli, M.; Balzani, V.; Lehn, J. M.; Zeissel, R.; Ungaro, R. *J. Lumin.* **1991**, *48&49*, 463. (b) Kawa, M.; Fréchet, J. M. J. *Chem. Mater.* **1998**, *10*, 286. (c) Bekiari, V.; Lianos, P. *Adv. Mater.* **1998**, *10*, 1455.

(34) (a) Klink, S. I.; Grave, L.; Reinhoudt, D. N.; van Veggel, F. C. J. M.; Werts, M. H. V.; Geurts, F. A. J.; Hofstraat, J. W. *J. Phys. Chem. A* **2000**, *104*, 5457. (b) Iwamuro, M.; Wada, Y.; Kitamura, T.; Nakashima, N.; Yanagida, S. *Phys. Chem. Chem. Phys.* **2000**, *2*, 2291.

(35) Lai, W. P. W.; Wong, W. T. *New J. Chem.* **2000**, *24*, 943.

(36) (a) Tsvirko, M. P.; Stelmakh, G. F.; Pyatosin, V. E.; Solovyov, K. N.; Kachura, T. F. *Chem. Phys. Lett.* **1980**, *73*, 80. (b) Asano-Someda, M.; Kaizu, Y. *J. Photochem. Photobiol. A* **2001**, *139*, 161.

(37) Dexter, D. L. *J. Chem. Phys.* **1953**, *21*, 836.

(38) Filipescu, N.; Sager, W. F.; Serafin, F. A. *J. Phys. Chem.* **1964**, *68*, 3324.

(39) Khreis, O. M.; Gilin, W. P.; Somerton, M.; Curry, R. J. *Org. Electron.* **2001**, *2*, 45.

(40) Reinhard, C.; Güdel, H. U. *Inorg. Chem.* **2002**, *41*, 1048.

(41) Regulacio, M. D.; Pablico, M. H.; Vasquez, J. A.; Myers, P. N.; Gentry, S.; Prushan, M.; Tam-Chang, S. W.; Stoll, S. L. *Inorg. Chem.* **2008**, *47*, 1512.

(42) (a) Wang, G. F.; Chen, W. Z.; Li, Z. B.; Hu, Z. S. *Phys. Rev. B* **1999**, *60*, 15469. (b) Hasegawa, Y.; Yamamuro, M.; Wada, Y.; Kanehisa, N.; Kai, Y.; Yanagida, S. *J. Phys. Chem. A* **2003**, *107*, 1697.

(43) (a) Soares-Santos, P. C. R.; Nogueira, H. I. S.; Félix, V.; Drew, M. G. B.; Ferreira, R. A. S.; Carlos, L. D.; Trindade, T. *Chem. Mater.* **2003**, *15*, 100. (b) Malta, O. L.; Couto dos Santos, M. A.; Thompson, L. C.; Ito, N. K. *J. Lumin.* **1996**, *69*, 77.

(44) (a) Wang, G. F. *J. Opt. Soc. Am. B* **2001**, *18*, 173. (b) Zheng, Z. Q.; Liang, H.; Ming, H.; Zhang, Q. J.; Xie, J. P. *Opt. Commun.* **2004**, *233*, 149.

(45) (a) Malta, O. L.; Carlos, L. D. *Quim. Nova* **2003**, *26*, 889. (b) Oomen, E. W. J. L.; van Dongen, A. M. A. *J. Non-Cryst. Solids* **1989**, *111*, 205. (c) Judd, B. R. *J. Chem. Phys.* **1979**, *70*, 4830.

(46) Koeppen, C.; Yamada, S.; Jiang, G.; Garito, A. F. *J. Opt. Soc. Am. B* **1997**, *14*, 155.

(47) Chen, X. Y.; Jensen, M. P.; Liu, G. K. *J. Phys. Chem. B* **2005**, *109*, 13991.

(48) Kumar, G. A.; Martinez, A.; Rosa, E. D. L. *J. Lumin.* **2002**, *99*, 141.

(49) (a) Rolli, R.; Gatterer, K.; Wachtler, M.; Bettinelli, M.; Speghini, A.; Ajo, D. *Spectrochim. Acta A* **2001**, *57*, 2009. (b) Becker, P. C.; Olsson, N. A.; Simpson, J. R. *Erbium-Doped Fiber Amplifiers: Fundamentals and Technology*; Becker, P. C. Ed.; Academic Press: San Diego, 1999.

JP9005179